Ocean Dynamics (2013) 63:447–457
DOI 10.1007/s10236-013-0601-9

# Waves, circulation and vertical dependence

**George Mellor**

Received: 4 August 2012 / Accepted: 31 January 2013 / Published online: 12 March 2013


**Abstract** Longuet-Higgins and Stewart (J Fluid Mech 13:481–504, 1962; Deep-Sea Res 11:529–562, 1964) and later Phillips (1977) introduced the problem of waves incident on a beach, from deep to shallow water. From the wave energy equation and the vertically integrated continuity equation, they inferred velocities to be Stokes drift plus a return current so that the vertical integral of the combined velocities was nil. As a consequence, it can be shown that velocities of the order of Stokes drift rendered the advective term in the momentum equation negligible resulting in a simple balance between the horizontal gradients of the vertically integrated elevation and wave radiation stress terms; the latter was first derived by Longuet-Higgins and Stewart. Mellor (J Phys Oceanogr 33:1978–1989, 2003a), noting that vertically integrated continuity and momentum equations were not able to deal with three-dimensional numerical or analytical ocean models, derived a vertically dependent theory of wave–circulation interaction. It has since been partially revised and the revisions are reviewed here. The theory is comprised of the conventional, three-dimensional, continuity and momentum equations plus a vertically distributed, wave radiation stress term. When applied to the problem of waves incident on a beach with essentially zero turbulence momentum mixing, velocities are very large and the simple balance between elevation and radiation stress gradients no longer prevails. However, when turbulence mixing is reinstated, the vertically dependent radiation stresses produce vertical velocity gradients which then produce turbulent mixing; as a consequence, velocities are reduced, but are still larger by an order of magnitude compared to Stokes drift. Nevertheless, the velocity reduction is sufficient so that elevation set-down obtained from a balance between elevation gradient and radiation stress gradients is nearly coincident with that obtained by the aforementioned papers. This paper includes four appendices. The first appendix demonstrates the numerical process by which Stokes drift is excluded from the turbulence stress parameterization in the momentum equation. A second appendix determines a bottom slope criterion for the application of linear wave relations to the derivation of the wave radiation stress. The third appendix explores the possibility of generalizing results by non-dimensionalization. The final appendix applies the basic theory to a problem introduced by Bennis and Ardhuin (J Phys Oceanogr 41:2008–2012, 2011).

**Keywords** Surface waves · Ocean circulation · Ocean modeling · Wave radiation stress

Responsible Editor: Leo Oey

This article is part of the Topical Collection on the *4th International Workshop on Modelling the Ocean in Yokohama, Japan 21–24 May 2012*

G. Mellor (✉)
Program in Atmospheric and Oceanic Sciences,
Sayre Hall, Forrestal Campus,
Princeton University, Princeton, NJ 08540-0710, USA
e-mail: glmellor@princeton.edu

## 1 Introduction

With few exceptions, three-dimensional numerical models of ocean dynamics ignore surface gravity wave interactions with the underlying currents. This paper presents a case for inclusion of wave dynamics in three-dimensional ocean models. All flow equations are phase-averaged which is necessary if one wishes to numerically model most ocean applications; otherwise, phase-resolved applications require time steps that are a fraction of wave periods.

There exist quite a few schemes for coupling surface gravity waves with the underlying ocean circulation. The earliest of these by Longuet-Higgins and Stewart (1960, 1962, 1964) and Phillips (1977) emphasized addition of a wave radiation stress term to the momentum equation to account for the effect of phase-averaged waves on currents. They obtained wave radiation stress terms from vertical integrals of linear wave properties. This writer has always considered their vertically integrated formulations to be correct. However, when it was deemed necessary to develop a wave-current formulation that could deal with vertically dependent underlying currents, the paper by Mellor (2003a) was created, features of which were: (1) The basic phase-averaged continuity and momentum equations—except for the addition of the wave radiation stress—were unchanged from the same equations with no waves so long as the total mean (Lagrangian) velocity was the (Eulerian) current plus Stokes drift. When vertically integrated, the equations agreed with that found in the earlier papers. (2) The vertically dependent, wave radiation stress, when vertically integrated, also agreed with the earlier papers.

Some readers will be aware that since the original 2003 paper, it has been necessary to twice revise the wave radiation stress part of the momentum equation; the continuity equation is unchanged. Rather than publish another corrigenda, I have deemed it useful to directly correct the original paper which can be found at ftp://aden.princeton.edu/pub/glm/corrected2003. It will be seen that the corrections are mainly related to a revised treatment of pressure as in Mellor (2011a). I do not anticipate further revision to Eqs. 1, 2, and 3 cited below.

### 1.1 The phase-averaged continuity equation

The continuity equation is

$$\frac{\partial DU_\beta}{\partial x_\beta}+\frac{\partial \Omega}{\partial \varsigma}+\frac{\partial \widehat{\eta}}{\partial t}=0, \tag{1}$$

It is convenient to use sigma coordinates, $(x_\alpha,\varsigma)$, such that the subscripts $\alpha$ or $\beta$ denote horizontal coordinates whereas the "sigma" independent variable, $\varsigma=(z-\widehat{\eta})/D$ (using $\varsigma$ instead $\sigma$, reserving the latter for frequency). The Cartesian vertical coordinate is $z$ and is positive upward. The mean elevation is $\widehat{\eta}$; $h$ is the bottom depth and $D\equiv\widehat{\eta}+h$. Further definitions are invoked: $u_{S\alpha}$ $(x_\alpha,\varsigma)$ is the Stokes drift (the phase-averaged flow due to waves). Similarly, $\widehat{u}_\alpha(x_\alpha,\varsigma)$ is the "current" (all other flows aside from those caused by waves) which is the usage in Phillips but is otherwise labeled "Eulerian current" in the literature. The sigma (nearly vertical) velocity is $\Omega$ and, in the absence of flow through bottom or surface (e.g., rain), $\Omega(0)=\Omega(-1)=0$.

The important aspect of (1) is that the continuity equation is unchanged from the equation without waves but is valid with waves so long as $U_\alpha=\widehat{u}_\alpha+u_{S\alpha}$.

### 1.2 The phase-averaged momentum equation

The momentum equation is more complicated and is

$$\frac{\partial DU_\alpha}{\partial t}+\frac{\partial}{\partial x_\beta}\left(DU_\beta U_\alpha+DS_{\alpha\beta}\right)+\frac{\partial \Omega U_\alpha}{\partial\varsigma}+\varepsilon_{\alpha\beta z}f_z DU_\beta + gD\frac{\partial\widehat{\eta}}{\partial x_\alpha}=\frac{\partial\tau_\alpha}{\partial\varsigma}, \tag{2a}$$

$$\tau_\alpha=\frac{K_M}{D}\frac{\partial\widehat{u}_\alpha}{\partial\varsigma}, \tag{2b}$$

wherein the boundary layer approximation has been invoked. The buoyancy term has been excluded from (2) since it is unchanged from the momentum equation without waves. In this paper, focus is on the radiation stress term which is

$$S_{\alpha\beta}=kE\left[\frac{k_\alpha k_\beta}{k^2}\frac{\cosh^2 kD(1+\varsigma)}{\cosh kD\sinh kD}-\delta_{\alpha\beta}\frac{\sinh^2 kD(1+\varsigma)}{\cosh kD\sinh kD}\right] + \delta_{\alpha\beta}\frac{E}{2D}\Im(\varsigma). \tag{3a}$$

$E$ is wave energy and $k$ is wave number.

The first two terms derive from $\overline{\widetilde{u}_\alpha\widetilde{u}_\beta}$ and $\overline{\widetilde{w}^2}$, respectively, where $\widetilde{u}_\alpha$ and $\widetilde{w}$ are obtained from the linear wave relations (see Appendix 2). The last term is

$$\Im(\varsigma)\equiv\frac{\partial}{\partial\varsigma}\left(2\frac{\cosh kD(1+\varsigma)\sinh kD(1+\varsigma)}{\cosh kD\sinh kD}-\frac{\sinh^2 kD(1+\varsigma)}{\sinh^2 kD}\right). \tag{3b}$$

The terms in the brackets relate to $\overline{\widetilde{p}\widetilde{s}}-g\overline{\widetilde{s}^2}/2$ where $\widetilde{s}$ is obtained from $\partial\widetilde{s}/\partial t=\widetilde{w}$.

Equation (3b) seems complicated, but the integral $\int_{-1}^{0}\Im(\varsigma)d\varsigma=1$ and for deep water (in practice $kD\geq3$ is sufficiently deep) $\Im(\varsigma)=2kD\exp(2kD\varsigma)=2kD\exp[2k(z-\widehat{\eta})]$. The function, $\Im(\varsigma)$, behaves like a Dirac delta function for large $k$. In Mellor (2011a), it was assumed to be a delta function for any $k$—this seemed to be a natural consequence of the methodology of Longuet-Higgins and Stewart (1964)—but was subject to criticism by by Aiki and Greatbatch (2013). The corrected Eq. (3b), now vertically variable, plays an important role in this paper. Aside from the treatment of (3b) , the Aiki and Greatbatch paper seems to have significant bearing on this paper but, I must confess, I don't understand the derivation of their basic equation nor do I perceive final results similar to (1), (2), and (3); they are needed to close the equation set for analytical or numerical application. In other words, the paper seems not to be finished.

Equation (2) includes a Reynolds stress term and an eddy viscosity, $K_M$. Note that the vertical velocity gradient in (2b) is $\partial\widehat{u}/\partial\varsigma$ rather than, say, $\partial U/\partial\varsigma$. Otherwise, the Stokes portion of $U$ would be subject to turbulent mixing and would conflict with that given by wave energy [see (9) and (11) below] and other wave properties. As demonstrated in Appendix 1, it is simple to accommodate (2b) numerically even though $U$ is the primary dependent variable in (1) and (2a).

Wave-to-circulation forcing in this paper is based on Eqs. 1, 2, and 3 and therefore differs, for example, from the derivations of McWilliams and Restrepo (1999) and Ardhuin et al. (2008). They deal with equations for the current (Eulerian) velocity rather than equations for the total mean (Lagrangian) velocity preferred here; it is sometimes described as the "vortex force formalism." When integrated vertically, their equations do not conform to the equations derived by Longuet-Higgins and Stewart (1964), Phillips (1977), and Smith (2006). Specifically, the treatment of pressure terms, as in Mellor (2011a) and now incorporated in the revised 2003 paper, are quite different; they lead to important components of the vertically dependent radiation stress. Bennis and Ardhuin (2011b) question the existence of a vertically variable radiation stress, as in (3b). This conflict is explored in Appendix 4.

This paper isolates the consequences of the wave radiation stress relations given by (3) and compares with results given by Longuet-Higgins and Stewart (1962) and Phillips (1977) for a somewhat idealistic problem. In contrast, a recent paper by Kumar et al. (2011) adopts the formulism of this paper and Mellor (2003a) to which, however, additional empiricism is added (e.g., wave breaking and rollers); their calculations compare favorably with data from the DUCK94 experiment (Feddersen et al. 1998) in water depths of 2 to 3 m. They also exclude Stokes drift from the turbulence stress term but in a more complicated but nevertheless equivalent way. The same data were modeled by Newberger and Allen (2007). Their model is also specialized to the surf zone and very shallow water where wave breaking is a dominant process. All wave processes are confined to an infinitesimally thin surface region wherein an integral interaction force is calculated and then, by assumption, distributed as a constant body force into the underlying water column. Uchiyama et al. (2010) and Kumar et al. (2012), using the vortex force formalism, also compare model results favorably with the DUCK 94 data; they also survey different empiricisms for processes such as wave breaking and surface rollers. Whereas the above papers deal with surf zone processes, the present paper is concerned with the interaction of the vertically variable radiation stress with bottom topography seaward of the surf zone.

Fundamental comparisons between the vortex force formalism and the radiation stress approach have not been broached (however, see the vertically integrated discussion by Smith 2006), but two differences are noted here: First, the vertical component of Stokes drift, $w_S$, following Longuet-Higgins and Stewart and Phillips, is zero in this paper, whereas it is non-zero in the vortex force formalism. Second, in the vortex force formalism, the momentum equation requires wave dissipation terms to account for transfer between Eulerian velocities and Stokes drift. In the present approach, this process is automatic since equations deal with combined Eulerian and Stokes velocities. Exclusion of Stokes drift in the turbulence shear term is explicit in the vortex force formalism.

## 2 A simple application

A classic problem involving wave–circulation interaction is that of a wave train incident on a sloping beach from deep to shallow water. It was treated by Longuet-Higgins and Stewart (1964) and later by Phillips (1977) wherein it was seen that the steady-state problem is reduced to algebra. Vertically integrated equations were used along with the reasonable assumption that velocities in the momentum advection term were of the order of Stokes velocities and therefore negligible compared to the barotropic pressure (elevation gradient) term and the wave radiation stress term. Consequently, the classic elevation set-down due to waves incident on a beach is obtained. Flow velocities are assumed to be Stokes flow at the surface plus a vertically constant reverse flow so that the vertically integrated flow is nil. Section 3 is a review of the solution by Longuet-Higgins and Stewart and Phillips which is then contrasted with the depth-dependent solution of Section 4. Wave breaking parameterizations are omitted; wave energy is absorbed at the shallow boundary.

If, instead of the vertically integrated momentum equation, one considers its vertically dependent counterpart, one is forced to conclude that the velocities in the advective term are not of the order of Stokes flow and are not negligible. This complicates the problem such that the simple (and elegant) algebraic solution reviewed in Section 3 may no longer be valid. A numerical solver is needed and is provided in Section 4. For (essentially) zero vertical mixing coefficient, one finds that, due to the vertically variable radiation stress term in the momentum equation, velocities and the advection term are very large relative to Stokes drift. Elevation set-down deviates significantly from the classic result of Longuet-Higgins and Stewart (1964) and Phillips (1977) and from measurements. However, inclusion of turbulence momentum transfer reduces velocities, although still an order of magnitude larger than Stokes drift, so that the advection term in the momentum equation is no longer competitive with the radiation and elevation gradient terms. The result is that elevation set-down reverts to the classic result—but for different physics—and conforms to the laboratory measurements of Bowen et al. (1968).

We do depart from Phillips' nomenclature using that which is more easily visualized (Smith 2006). To focus on the changes due to the vertically dependent continuity and momentum equations, attention is confined to unidirectional, planer ($x$, $\varsigma$) flow. Thus, to be clear about the problem setup, Eqs. (1), (2), and (3) are appropriately simplified so that

$$\frac{\partial DU}{\partial x}+\frac{\partial \Omega}{\partial \varsigma}+\frac{\partial \widehat{\eta}}{\partial t}=0, \tag{4}$$

and

$$\frac{\partial DU}{\partial t}+\frac{\partial DU^2}{\partial x}+\frac{\partial \Omega U}{\partial \varsigma}+\frac{\partial DS_{xx}}{\partial x}+gD\frac{\partial \widehat{\eta}}{\partial x}=\frac{\partial \tau}{\partial \varsigma}; \tag{5a}$$

$$\tau=\frac{K_M}{D}\frac{\partial \widehat{u}}{\partial \varsigma}. \tag{5b}$$

To conform to the Phillips problem, zero surface and bottom stress is stipulated so that

$$\tau(0^+)=\tau(-1)=0. \tag{6}$$

Restricting attention to planar flow and monochromatic waves, the vertically dependent wave radiation stress term, (3), simplifies to

$$S_{xx}=\frac{2kE}{\sinh 2kD}+\frac{E}{2D}\Im(\varsigma). \tag{7}$$

The definition of $\Im$ is unchanged from (3b). In (7), $k$ is the wave number; $E$ is the wave energy such that $E=g\overline{\widetilde{\eta}^2}$ where $g$ is the gravity constant; $\widetilde{\eta}$ is the instantaneous wave elevation, and the overbar signifies phase averaging.

The wave number, $k$, is obtained from the dispersion relation,

$$\sigma^2=kg\tanh kD, \tag{8}$$

where the wave frequency,$\sigma$, is constant; therefore $k(x)$ is only dependent on $D(x)$.

The wave energy equation is

$$\frac{\partial E}{\partial t}+\frac{\partial}{\partial x}\left[(c_g+u_A)E\right]+\int_{-1}^{0}S_{xx}\frac{\partial U}{\partial x}Dd\varsigma=0 \tag{9}$$

wherein the group speed is

$$c_g=\frac{\partial \sigma}{\partial k}=\frac{c}{2}\left(1+\frac{2kD}{\sinh 2kD}\right), \tag{10}$$

and $c=\sigma/k$ is the phase speed. The advective term is $u_A=k\int_{-1}^{0}rUDd\varsigma$ and $r$ is a weighting function confined to the near surface and $k\int_{-1}^{0}rDd\varsigma=1$; in deep water, $r=2\exp(2kD\varsigma)$; otherwise, hyperbolic functions are needed. To simplify the problem and to relate to Phillips' solution, source and sink terms—and, thus, wave breaking parameterizations—have been excluded in (9).

After calculating $E$, $k$, and $c=\sigma/k$ from the above equations, Stokes drift is obtained from

$$u_S=-\frac{2kE}{c}\frac{\cosh 2kD(\varsigma+1)}{\sinh 2kD}, \tag{11}$$

as derived in many papers (e.g., Phillips 1977; see Mellor 2003a for an alternate derivation).

## 2.1 The vertically integrated equations

An advantage of sigma coordinates is that boundary conditions, $\Omega(0)=\Omega(-1)=0$, are "built in" to (4) and (5a, b) which can be integrated very simply. Thus, if one integrates (4) and (5a, b) from $\varsigma=-1$ to $\varsigma=0$, the results subject to (6) are

$$\frac{\partial M}{\partial x}+\frac{\partial \widehat{\eta}}{\partial t}=0, \tag{12}$$

and

$$\frac{\partial M}{\partial t}+\frac{\partial}{\partial x}\int_{-1}^{0}DU^2d\varsigma+\frac{\partial \overline{S}^z_{xx}}{\partial x}+gD\frac{\partial \widehat{\eta}}{\partial x}=0, \tag{13}$$

where

$$M(x)\equiv\int_{-1}^{0}UDd\varsigma. \tag{14}$$

Note that $\int_{-1}^{0}(\ )Dd\varsigma=\int_{-h}^{\widehat{\eta}}()dz$. Upon integrating (7),

$$\overline{S}^z_{xx}\equiv\int_{-1}^{0}S_{xx}Dd\varsigma=E\left(2\frac{c_g}{c}-1\right)+\frac{E}{2}. \tag{15}$$

The expression on the right of (15) has been separated into two terms so as to relate to the first and second terms on the right of (7). They, of course, combine so that $\overline{S}^z_{xx}=E\times\left(2c_g/c-1/2\right)$. In deep water, $c_g/c=1/2$ and $\overline{S}^z_{xx}=E/2$, whereas in shallow water, $c_g/c=1$ and $\overline{S}^z_{xx}=3E/2$.

# 3 Analysis using vertically integrated equations

In this section, we review the idealistic problem in Longuet-Higgins and Stewart (1964), Phillips (1977), and Xu and Bowen (1994) whereby an offshore wave train is incident on a beach. There is no wind and attention is restricted to the case where the waves are normal to the shoreline. The following definitions are invoked: $M_S(x)\equiv\int_{-h}^{\widehat{\eta}}u_Sdz$ and $\widehat{M}(x)\equiv\int_{-h}^{\widehat{\eta}}\widehat{u}dz$. As previously defined, the total mean velocity is $U=\widehat{u}+u_S$ so that $M=\widehat{M}+M_S$. For steady flow and flow normal to a closed boundary,

$$M = 0 \text{ and } \widehat{M} = -M_S, \tag{16}$$

where $\widehat{M}$ is predominantly an undercurrent.

*If*, as in Phillips, it is assumed that $U$ is of the order of Stokes drift, then it can be shown that the wave energy Eq. (9) reduces to

$$\frac{\partial(c_g E)}{\partial x} = 0, \tag{17}$$

The other terms in (9) are of order $(ka)^2$ smaller than (17); $k$ is the wave number; $a$ is the wave amplitude. For monochromatic waves, $\sigma(x)=\sigma_\infty$ where the subscript, $\infty$, denotes quantities far offshore (where $kD>>1$). Since $c \equiv \sigma/k$, a combination of (10) and (17) yields

$$\frac{E_\infty}{E} = \frac{k_\infty D}{kD}\left(1 + \frac{2kD}{\sinh 2kD}\right), \tag{18}$$

and from (8)

$$kD \tanh kD = k_\infty D. \tag{19}$$

Figure 1a contains plots derived from (18) and (19).

Thus far, only the wave energy equation and the continuity equation have been used. However, again assuming that $U$ is of the order of Stokes drift, the momentum Eq. (13) reduces to

$$\frac{\partial \overline{S}^{z}_{xx}}{\partial x} = -gD\frac{\partial \widehat{\eta}}{\partial x}. \tag{20}$$

Combining (15) and (20) one obtains

$$\frac{g d\widehat{\eta}}{k_\infty E_\infty} = -\frac{1}{k_\infty D} d\left[\frac{E}{E_\infty}\left(2\frac{c_g}{c} - \frac{1}{2}\right)\right]. \tag{21}$$

Using (10), (18), and (19), Eq. (21) can be integrated and $g\widehat{\eta}/k_\infty E_\infty$ is shown in Fig. 1b (and in Fig. 3.5 of Phillips).

Phillips assumed $\widehat{u} = \widehat{M}/D = -M_S/D$ to be independent of $z$. The vertically dependent Stokes speed is given by (11) and its vertical integral is $M_S = -E/c$ so that $\widehat{u} = E/(cD)$. Thus, by assumption, the flow field is given by

$$U(x,z) = E/(cD) + u_S. \tag{22}$$

Figure 2 is a plot of (22) for $kD$=3.0, a value sufficiently large to be considered deep water flow in which case $u_S \cong -(2kE/c)\exp(2kD\varsigma)$. As $x$ decreases from deep to shallow water, so does $kD$ and the entire, depth dependent flow field is determined from (11), (22) and wave properties $E$, $k$, and $c$.

In the following section, it will be found that, contrary to (22), $\widehat{u}$ is dependent on $\varsigma$ and $u_S(x,\varsigma) << \widehat{u}(x,\varsigma)$.

## 4 Calculations using vertically dependent equations

We now treat the same problem as above; the bottom, $h(x)$, however, is specialized to have a constant slope. The

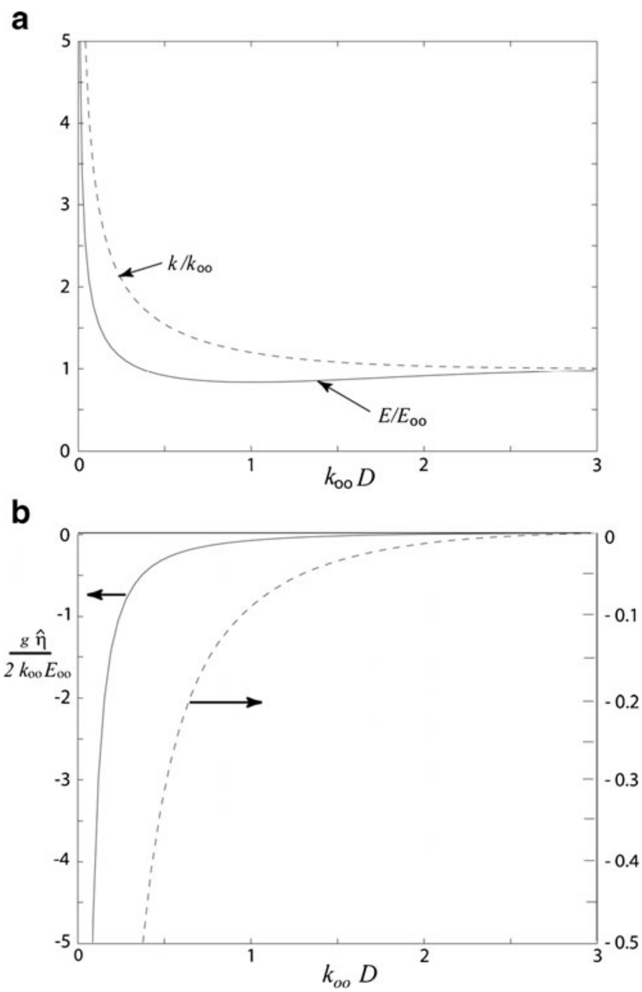


**Fig. 1** **a** The variation of wave energy and wave number as function of water column depth according to Phillips (1977). **b** The set-down of surface elevation as a function of water column depth according to Phillips (1977)

advective or turbulence-viscous terms in (5a, b) can no longer be ignored; they are needed to balance the vertical variability of $S_{xx}$ ($x$, $\varsigma$). A numerical model is needed for which the Princeton Ocean Model (Blumberg and Mellor 1987; Mellor 2003b) is used. The horizontal grid increment is 25 m, and there are 21 sigma increments evenly spaced except near the surface where the first seven grid points are logarithmically distributed. To eliminate $2\Delta x$ noise, a horizontal diffusion term $A\partial(2\partial U/\partial x)/\partial x$ is added to the right side of (2a). The coefficient, $A$=0.25 $m^2 s^{-1}$, is sufficiently small so that, in the ensuing calculations, diagnostics show the diffusion term to be approximately three orders of magnitude smaller than, say, the forcing term, $\partial(DS_{xx})/\partial x$ in (5a, b).

The circulation model was coupled to the numerical version (simplified from Mellor et al. 2008) of Eq. 9. The entering boundary conditions at a depth of 50 m are $E$=2.4 $m^3 s^{-2}$ ($H_S$=2.0 m), σ=0.766 $s^{-1}$ for which $k$=0.060 $m^{-1}$.

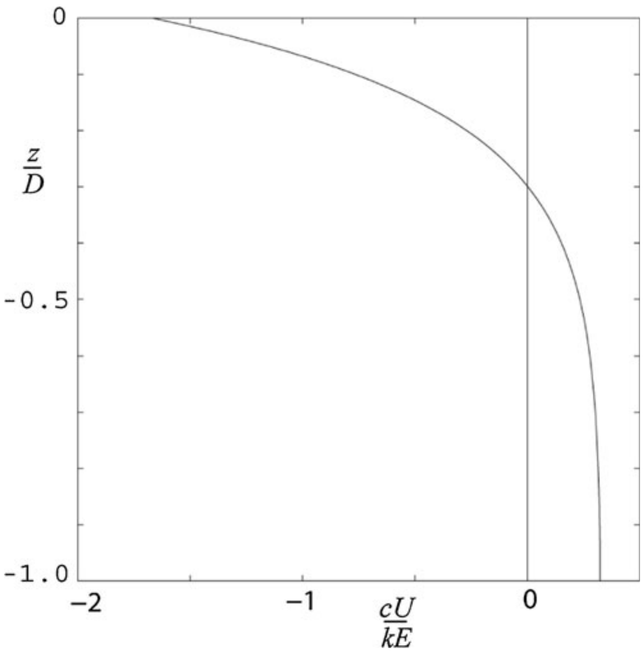


**Fig. 2** The non-dimensional mean velocity (Stokes plus current) profile implied by Phillips (1977); Eq. (22) for $kD$=3

4.1 Solutions with $K_M$>0

Figure 3 shows the results of the calculation—integrated in time until steady state is attained—with a sloping bottom described above. Wave energy varies according to (9) as shown in Fig. 3a. It is absorbed at the otherwise closed boundary at $x$=0 and is affected by inclusion of the terms $u_A$ and the last term on the left of (9), but the effects are small and wave energy varies very nearly as in Section 3. The wave number varies in the same way as in Section 3 since it is dependent only on depth as seen in (19).

Figure 3b shows contours of $K_M$ calculated according to the Mellor and Yamada (1982) closure model—shown to successfully model different neutral turbulent flow applications (and thence stratified flows) such that $K_M$=$S_M \ell q$ where, for zero stratification, $S_M$=0.39; $q^2$ is obtained from the solution of the turbulence kinetic equation and $\ell$ from a similar length scale equation; however, at the surface $\ell$ is proportional to significant wave height as in Mellor and Blumberg (2004).

In Fig. 3c, since $U$ is non-divergent ($\hat{u}$ and $u_S$ separately are divergent), stream function contours ($\partial\Psi/\partial\varsigma = DU$, $\partial\Psi/\partial x = -\Omega$) are shown. A profile, $U(\varsigma)$, is also shown where velocity is maximum. The maximum total current is 0.21 ms$^{-1}$ in contrast to the maximum Stokes drift, 0.020 ms$^{-1}$. Thus, the total mean velocities in Fig. 3c depart markedly from the sample profile in Fig. 2 and for similar profiles for varying $kD$.

The calculated set-down in Fig. 3d differs from that obtained from (21) or Fig. 1b but by a nearly negligible amount. In the integrated momentum Eq. (13), the last two terms on the left dominate as will be detailed in Fig. 5.

Consideration of wave breaking in shallow water is excluded in this paper as it was by Longuet-Higgins and Stewart (1964) and by Phillips (1977). However, incipient breaking in the surf zone with mild slope can be estimated according to $a/h \cong 0.4$ (Dean and Dalrymple 1998) where $a = (2E/g)^{1/2}$. In Fig. 4, this would occur in depths of about 2 m and, thus, cannot be resolved in this calculation.

Results such as Fig. 3 depend on $K_M(x,\varsigma)$. However, a calculation (not shown) with $K_M$ = constant = 0.040m$^2$s$^{-1}$ is very similar to Fig. 3 but with higher velocities in the shallowest water.

4.2 Solutions for $K_M \cong 0$

The solution of Longuet-Higgins and Stewart (1964) and Phillips (1977) posited $K_M$=0. Therefore, calculations from the corresponding numerical solution are shown in Fig. 4 for $K_M \cong 0$ (Using $K_M$=0.0 produced some noise so a very small value, $K_M$=0.005 m$^2$s$^{-1}$, was used to obtain a more attractive figure). The velocities are much larger than that for $K_M$> 0 particularly near the bottom where the undertow is confined to a thin layer. Since squared velocities are involved in the advective term in (5a, b), the elevation set-down is significantly affected as shown in Fig. 4b.

Figure 5 presents the vertically integrated balance of terms showing that, in Fig. 5a, the advective term for $K_M$> 0 is small and does not compete with the horizontal gradients of radiation stress or elevation. For $K_M \cong 0$, the advective term is significant as shown in Fig. 5b. Thus, whereas $K_M \cong 0$ formulation is idealistically closer to the formulation of Longuet-Higgins and Stewart (1964) and Phillips (1977), it disagrees with their elevation set-down and with the laboratory measurements by Bowen et al. (1968). Close set-down agreement is obtained for $K_M$> 0.

## 5 Range of validity for sloping bottoms

A question arises as to whether it is appropriate to use linear wave relations as the basis of the wave radiation stress derivation in problems where the bottom is sloped as in this paper. To resolve this question, it is shown in Appendix 2 that $(\partial h/\partial h/sinhkD)^2$ should be small and of the order $(ka)^2$ or less where $(ka)^2$ must be small ab initio. Notice that the $\sinh^{-1}kD$ factor allows for steep slopes in deep water in accordance with intuition.

In the example in this paper, $\partial h/\partial x = 0.05$. Referring to Fig. 3 where $D$=50 m, $k$=0.060 m$^{-1}$, $a$=0.70 m so that $(ka)^2 = 2 \times 10^{-3}$ and $(\partial h/\partial x/\sinh kD)^2 = 2 \times 10^{-5}$. Where $D$=10 m, $k$=0.08 m$^{-1}$, $a$=0.65 m so that $(ka)^2 = 3 \times 10^{-3}$ and $(\partial h/\partial x/\sinh kD)^2 = 3 \times 10^{-3}$.

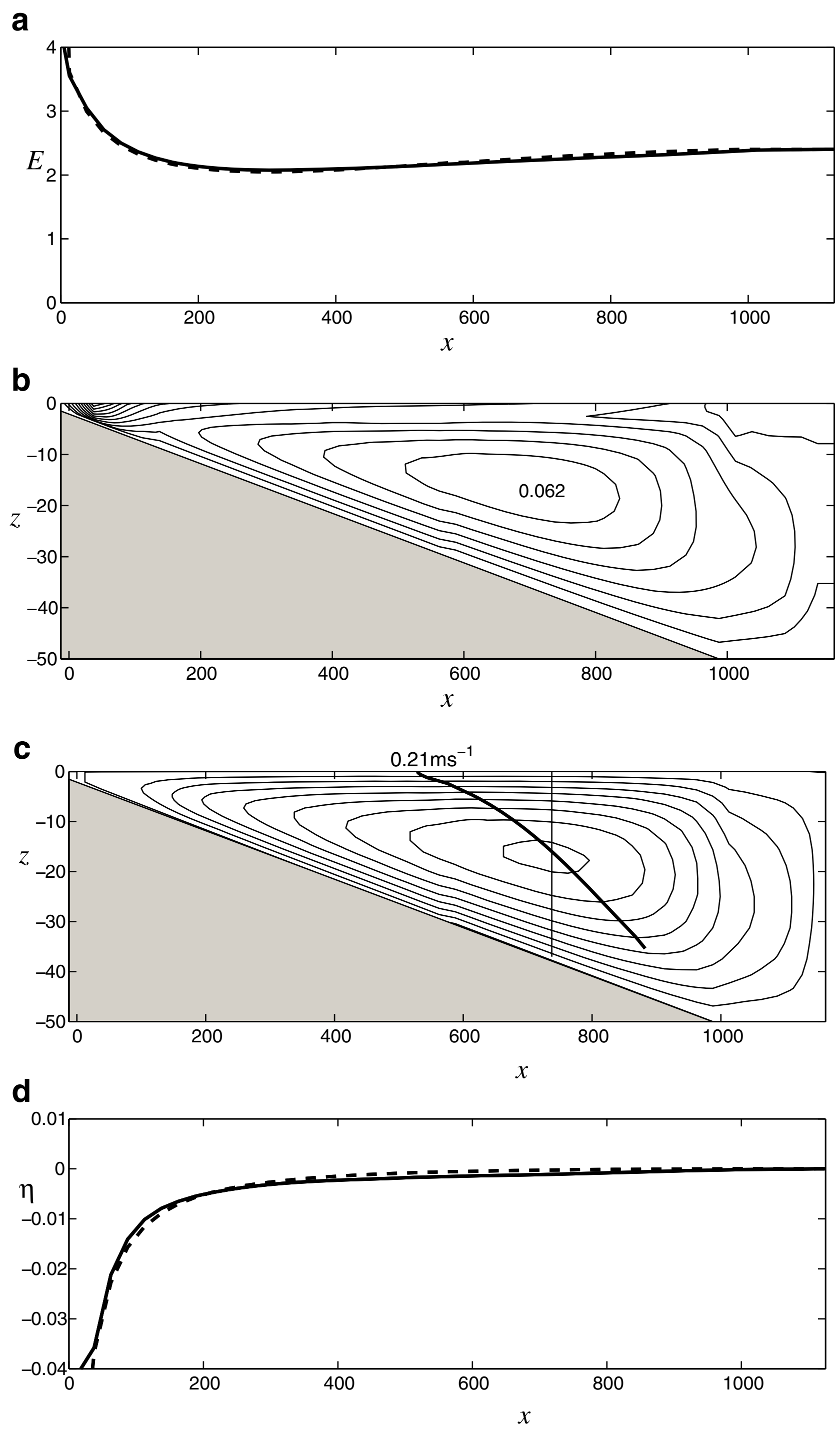


**Fig. 3** **a** The variation in wave energy, $E$/m$^3$s$^{-2}$. The *solid line* is calculated according to (6); the *dashed line* is according to (14) as in Fig. 1a. **b** The vertical mixing coefficient, $K_M$; the contour interval is 0.01 m$^2$s$^{-1}$. **c** The mean velocity stream function $(\partial\Psi/\partial\varsigma = DU,\ \partial\Psi/\partial x = -\Omega)$; the contour interval is 0.2 m$^2$s$^{-1}$. The mean velocity profile is the *heavy line*; the maximum value is about ten times that of Stokes drift. **d** The elevation, $\widehat{\eta}$/m. The *solid line* is according to (2); the *dashed line* is from (17)

## 6 Summary

The approach of Mellor (2003a) is the same as Longuet-Higgins and Stewart (1962, 1964) and Phillips (1977) in that one deals with continuity and momentum equations wherein velocity is the sum of the current plus Stokes drift. Their theory, based on vertically integrated equations and negligible advection in the momentum equation, yields the simple algebraically derived, classic elevation set-down result. However, the assumption that the flow field is only comprised of Stokes drift plus a compensating vertically constant current can lead to significant errors in the flow field.

Alternately, the development of vertically dependent continuity, momentum equations, and a depth-dependent radiation stress described in this paper requires a numerical model and turbulence mixing of momentum. Nevertheless, the classic elevation set-down is obtained and conforms to the laboratory measurements of Bowen et al. (1968).

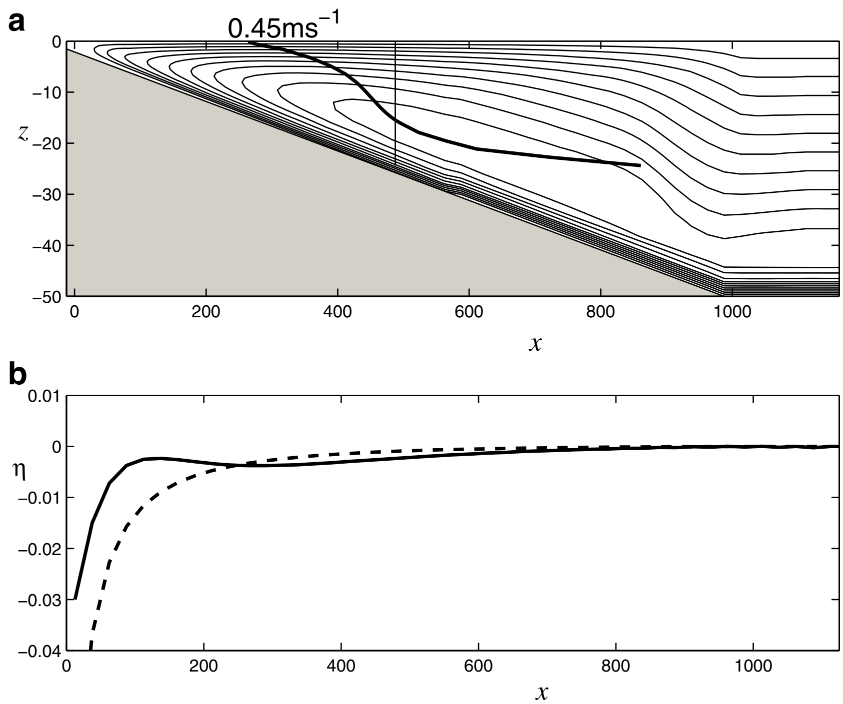


**Fig. 4** The same as Fig. 3c, d except that $K_M$ is essentially zero. Unlike Fig. 3d, the calculated elevation does not coincide with the analytical expression obtained from Eq. (21)

However, if turbulence mixing is excluded, velocities (Stokes drift plus larger currents) are large resulting in elevation set-down departures from the classic result.

Since Stokes drift is governed by wave energy and the other wave properties, it must be excluded from momentum mixing. Appendix 1 shows how this can be handled in the numerical model deployed in this paper which otherwise deals primarily with the sum of Stokes drift and currents. The vertically dependent, wave radiation stress uses well-known linear wave relation which are derived assuming a flat bottom. Appendix 2 develops a criterion for their application to sloping bottoms. The possibility of making computed results non-dimensional and, thus, more general is examined in Appendix 3. In Appendix 4, a shallow water problem introduced by Bennis and Ardhuin is discussed. Implicit is their assumption of a vertically constant radiation

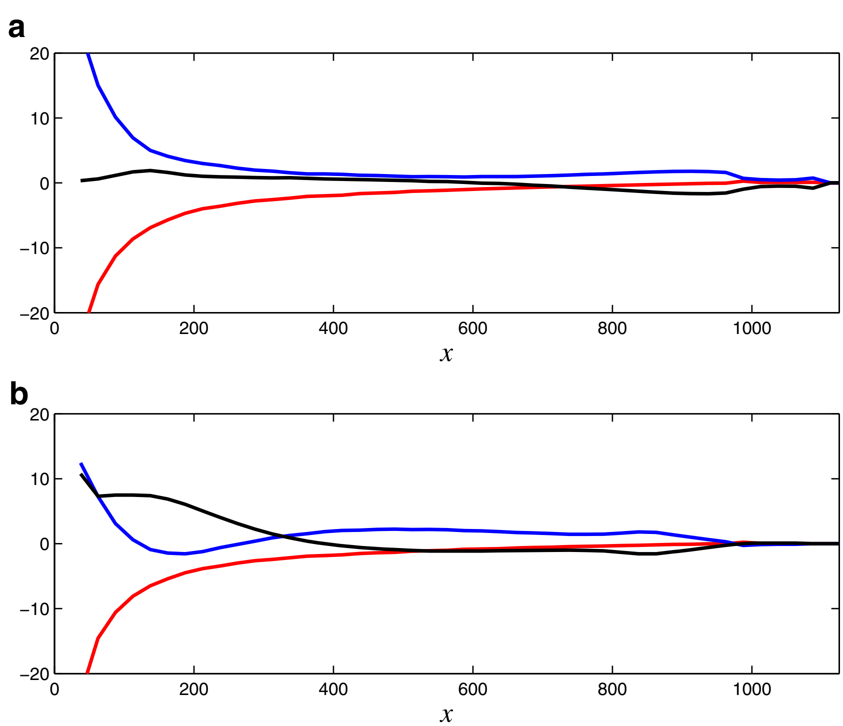


**Fig. 5** Diagnostics of the vertically integrated terms in (13). The *black lines* are $\partial\left(\int_{-1}^{0} DU^2 d\varsigma\right)/\partial x$; the *red lines* are $\partial\overline{S}_{xx}^{\tilde{z}}/\partial x$ and the *blue lines* are $gD\partial\widehat{\eta}/\partial x$. The calculation ran to steady state. All quantities are to be multiplied by $1 \times 10^{-3}\mathrm{m}^2\mathrm{s}^{-2}$; they sum to zero within round-off error. Notice that the integral of $\partial\tau/\partial\varsigma$ is nil due to (6). **a** Diagnostics corresponding to Fig. 3 wherein $K_M$ is according to Fig. 3b. **b** Diagnostics corresponding to Fig. 4 wherein $K_M$ is essentially zero

stress which, as might have been anticipated from results in the main text, differs significantly from results using a vertically variable radiation stress relation.

**Acknowledgments** Comments by reviewers were helpful in revising the paper.

## Appendix 1

A simple test of numerical accuracy and the stress term in (2b)

In order to test the code where the vertical mixing is according to Mellor and Yamada (1982) and which is here modified so that $u_S$ is excluded from velocity shear determination as in (2b), we first consider a flat "beach" with swell entering the upstream boundary given by the wave parameters cited in Section 4. Wave energy is maintained constant so that gradients of the radiation stress are nil. Of course, in a phase-averaged formulation, the only manifestation of swell is the accompanying Stokes drift. It is noted that Stokes drift is created by that portion of surface wind stress due to pressure-slope forcing (Donelan 1999; Mellor 2003a). In this case of zero wind, Stokes drift is created upstream of the region considered here. The entering flow is given by (11) plus a vertically constant offshore current, $\widehat{M}/D$, necessary to satisfy $M$=0. The calculation in Fig. 6, after reaching steady state and presented in the form of a stream function, demonstrates that the Stokes drift is not diffused so that $U(x,\varsigma) \cong u_S(\varsigma) + \widehat{M}/D$ everywhere except near the closed end ($x$<200 m) where horizontal diffusion is necessarily manifest; at $x$=0, $U(0,\varsigma)$=0.

A calculation was also executed (not shown) where $U$ was inserted into (2b) instead of $\widehat{u}$. As anticipated, the Stokes flow diffused vertically and decayed significantly downstream of $x\cong$1000m contrary to Eq. (11) for constant $E$.

Notice that the numerically generated profile in Fig. 6 closely approximates the analytical profile in Fig. 2 attesting to the accuracy of the numerical solution as does Fig. 3a or d.

## Appendix 2

The linear wave solutions with bottom slope

The governing equation for irrotational flow is

$$\phi_{xx} + \phi_{yy} + \phi_{zz} = 0, \quad \text{(B – 1)}$$

whose solution we take to be the real part of

$$\phi = \left(Ae^{kz} + Be^{-kz}\right)ie^{i\psi}, \qquad \psi \equiv k_\alpha x_\alpha - \sigma t, \quad \text{(B – 2a, b)}$$

and the surface wave elevation is the real part of

$$\widetilde{\eta} = ae^{i\psi}, \quad \text{(B – 3)}$$

where $a = a(x_\alpha, t)$ varies on spatial and temporal scales which are large compared to $k^{-1}$ and $\sigma^{-1}$, respectively.

The surface boundary condition is $\partial\phi/\partial z|_{\widehat{\eta}} = \partial\widetilde{\eta}/\partial t$. Thus, from (B-2a) and (B-3)

$$Ae^{\widehat{\eta}} - Be^{-\widehat{\eta}} = -\frac{a\sigma}{k}. \quad \text{(B – 4)}$$

At the bottom, $\partial\phi/\partial z|_{-h} = -\partial\phi/\partial x_\alpha|_{-h}(\partial h/\partial x_\alpha)$ and one obtains from (B-2a)

$$B = Ae^{-2kh}\frac{1+if}{1-if}, \quad \text{(B – 5)}$$

where $f$ is defined by

$$f \equiv \frac{k_\alpha}{k}\frac{\partial h}{\partial x_\alpha}. \quad \text{(B – 6)}$$

Now insert (B-4) and (B-5) into (B-2a) and let $f$<<1. After considerable algebra, the real part of (B-2a) is

$$\phi = ac\frac{\cosh k(z+h)}{\sinh kD}\sin\psi + \frac{f}{\sinh kD}ac \times \frac{\cosh k(z-\widehat{\eta})}{\sinh kD}\cos\psi. \quad \text{(B – 7)}$$

where the relation, $\cosh k(z+h)\cosh kD - \sinh k(z+h) \times \sinh kD = \cosh k(z-\widehat{\eta})$ has been used and $D \equiv \widehat{\eta} + h$.

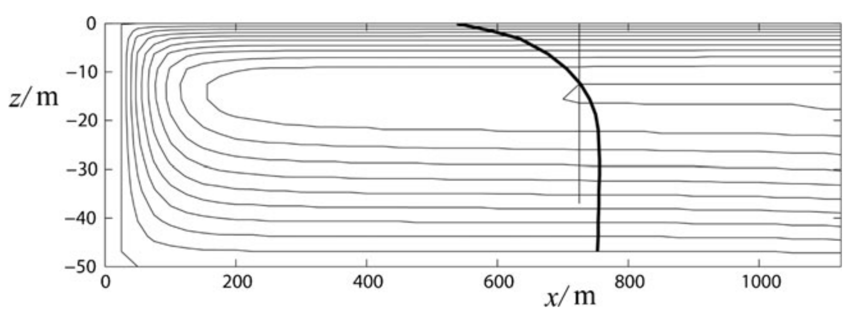


**Fig. 6** Illustration of the fact that the POM code has been modified so as to exclude vertical mixing due to Stokes drift. The stream function contour interval is 0.01 $m^2 s^{-1}$. The *heavy line* is a velocity profile; the maximum velocity is 0.020 $ms^{-1}$ and is everywhere dominated by the upstream boundary condition $\left[U(x,\varsigma) \cong u_S(\varsigma) + \widehat{M}/D\right]$ except in the region, 0<$x$<200 m, where departures from horizontal homogeneity are due to horizontal diffusion. The numerically generated profile in this figure very nearly coincides with the analytical profile in Fig. 2

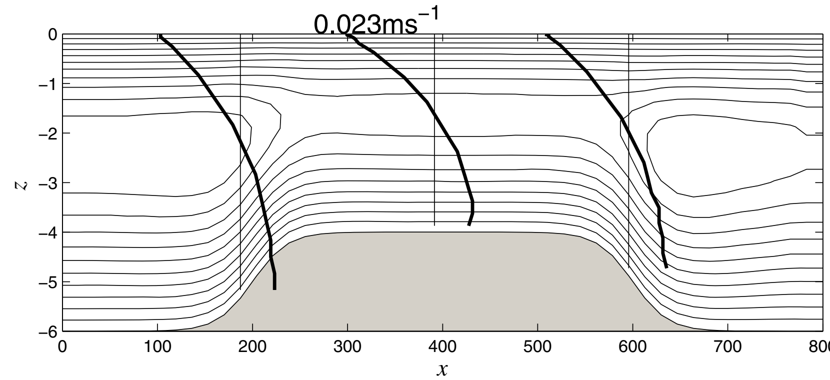


**Fig. 7** The shallow water ($kD \cong 1$) solution with a vertically constant radiation stress according to Bennis and Ardhuin (2011). The waves progress from right to left. The flow is essentially Stokes drift plus a compensating vertically constant current; the turbulent mixing is nil due to (5a, b). The stream function contour interval is 0.002 $m^2s^{-1}$

The velocity components, $(\widetilde{u}_\alpha, \widetilde{w}) = (\partial\phi/\partial x_\alpha, \partial\phi/\partial z)$, are

$$\widetilde{u}_\alpha = \frac{k_\alpha}{k} akc\left\{\frac{\cosh k(z+h)}{\sinh kD}\cos\psi - \frac{f}{\sinh kD}\frac{\cosh k(z-\widehat{\eta})}{\sinh kD}\sin\psi\right\}, \tag{B-8a}$$

and

$$\widetilde{w} = akc\left\{\frac{\sinh k(z+h)}{\sinh kD}\sin\psi + \frac{f}{\sinh kD}\frac{\sinh k(z-\widehat{\eta})}{\sinh kD}\cos\psi\right\}, \tag{B-8b}$$

so that the phase averaged stresses are

$$\overline{\widetilde{u}_\alpha\widetilde{u}_\beta} = \frac{k_\alpha k_\beta}{k^2}\frac{(ka)^2c^2}{2} \times\left\{\frac{\cos\mathrm{h}^2\, k(z+h)}{\sin\mathrm{h}^2\, kD} - \left(\frac{f}{\sinh kD}\right)^2\frac{\cos\mathrm{h}^2\, k(z-\widehat{\eta})}{\sin\mathrm{h}^2\, kD}\right\}, \tag{B-9a}$$

$$\overline{\widetilde{u}_\alpha\widetilde{w}} = 0, \tag{B-9b}$$

and

$$\overline{\widetilde{w}^2} = \frac{(ka)^2c^2}{2} \times\left\{\frac{\sin\mathrm{h}^2\, k(z+h)}{\sin\mathrm{h}^2\, kD} + \left(\frac{f}{\sinh kD}\right)^2\frac{\sin\mathrm{h}^2\, k(z-\widehat{\eta})}{\sin\mathrm{h}^2\, kD}\right\}. \tag{B-9c}$$

The only part of (B-9) that is used in this paper is the fact that $(f/\sinh kD)^2$ must be small in order to neglect the second terms in (B-9a) and (B-9c) in which case the first terms may be used for a sloping bottom.

## Appendix 3

Non-dimensional solutions

The results in Section 3 are non-dimensional and quite general. However, the results in Fig. 3 or 4 can only be partially generalized by normalizing $E$ by $E_\infty$, $x$ and $z$ by $K_\infty$, $k$ by $k_\infty^{-1}$, $U$ by $(k_\infty E_\infty)^{-1/2}$, $K_M$ by $k_\infty^{-1}(k_\infty E_\infty)^{-1/2}$, and $\widehat{\eta}$ by $g(k_\infty E_\infty)^{-1}$ for a given parameter, $\widetilde{E} = (k_\infty E_\infty)^{1/2}/c_\infty$ and for a specific $dh/dx = fcn(x)$. Velocities, for example, can be made non-dimensional according to

$$\frac{U}{(k_\infty E_\infty)^{1/2}} = \frac{\widehat{u}}{(k_\infty E_\infty)^{1/2}} + \frac{u_S}{(k_\infty E_\infty)^{1/2}} = \frac{\widehat{u}}{(k_\infty E_\infty)^{1/2}} + \widetilde{E}\left(\frac{k}{k_\infty}\right)^2\frac{E}{E_\infty} \times\frac{2\cosh 2kD(1+\varsigma)}{\sinh 2kD}.$$

Thus, results depend on the parameter, $\widetilde{E}$.

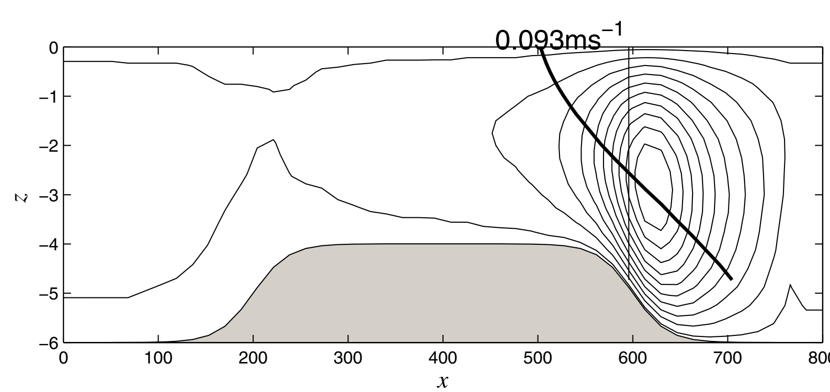


**Fig. 8** The shallow water ($kD \cong 1$) solution with a vertically variable radiation stress. The waves progress from right to left. The generated $\widehat{u}(x,\varsigma)$ is large compared to Stokes drift and turbulent mixing is significant. The stream function contour interval is 0.020 $m^2s^{-1}$

Calculations (not shown) were executed for $dh/dx = 0.05$ and $\widetilde{E} = 0.030$ and $\widetilde{E} = 0.060$. It was found that the sensitivity of the non-dimensional variables to variations of $\widetilde{E}$ is weak since $u_s << \widehat{u}$.

## Appendix 4

The test case of Bennis and Ardhuin

In objecting to my earlier representing (3b) as a Dirac delta function to which I now agree [but see my reply in Mellor (2011b)], Bennis and Ardhuin (2011) cite a case of flow in a converging, diverging free surface channel where waves enter one end of the channel; the flow is inviscid. The entering waves are shallow water waves such that $kD \cong 1.0$. The calculation in Fig. 7 is for vertically constant $S_{xx}$ as in (15). The entering total flow is Stokes flow plus a vertically constant flow, $\widehat{u}(x)$, scaled so that the vertical integral of the total flow is nil. The velocity profiles vary only slightly in passage through the channel. Although plotted differently, Fig. 7 reproduces the calculation of Bennis and Ardhuin which they termed the “exact solution.” Thus, the flow is that which was discussed in Section 3 corresponding to Figs. 1a, b and 2; it is in effect a special case of the more general solution by Longuet-Higgins and Stewart (1964) and Phillips (1977).

In contrast is the solution in Fig. 8 for vertically variable $S_{xx}$ according to (7). Initially, vertically variable, Eulerian velocities, $\widehat{u}$, large relative to Stokes drift, are created ($x \cong 600$ m) by vertically and horizontally varying, radiation stress gradients which are then subject to turbulence mixing ($x < 600$ m). Also, calculations (not shown) for $kD = 5$ were executed wherein waves do not “feel” the bottom; i.e., $S_{xx} = kE \exp[2k(z - \widehat{\eta})]$ and $\widehat{u}$ is small relative to Stokes drift and provides the vertically constant, return flow.

The important point is not whether (3b) is concentrated at the surface as in a delta function, rather whether it is vertically constant or not.

## References


Aiki H, Greatbatch RJ (2013) The vertical structure of the surface radiation stress for circulation over a sloping bottom as given by thickness-weighted-mean theory. J Phys Oceanogr 41:149–164

Ardhuin F, Rascle N, Belibassakis KA (2008) Explicit wave-averaged primitive equations using a generalized Lagrangian mean. Ocean Modelling 20:35–60

Bennis A-C, Ardhuin F (2011) Comments on “The depth-dependent current and wave interaction equations: a revision”. J Phys Oceanogr 41:2008–2012

Blumberg AF, Mellor GL (1987) A description of a three-dimensional coastal ocean model. Coastal Estuarine Science 4:1–16

Bowen AJ, Inman DL, Simmons VP (1968) Wave 'set-down' and set-up. J Geophys Res 73:2569–2577

Dean RG, Dalrymple RA. 1998: *Water wave mechanics for engineers and scientists*. Vol. 2, *Advanced Series on Ocean Engineering*, World Scientific, 353 pp

Donelan MA (1999) Wind-induced growth and attenuation of laboratory waves. In: Wind-over-wave couplings. Clarendon Press, Oxford, pp 183–194

Feddersen F, Guza RT, Elgar S, Herbers THC (1998) Alongshore momentum balances in the nearshore. J Geophys Res 103:15,667–15,676

Kumar N, Voulgaris G, Warner JC (2011) Implementation and modification of a three-dimensional wave radiation stress for surf zone and rip-current applications. Coastal Eng 58:1097–1117

Kumar N, Voulgaris G, Warner JC, Olabarrieta M (2012) Implementation of the vortex force formalism in the coupled ocean-atmosphere-wave-sediment transport (COAWST) system for inner shelf and surf zone application. Ocean Modelling 47:65–95

Longuet-Higgins MS, Stewart RW (1960) Changes in the form of short gravity waves on long waves and tidal streams. J Fluid Mech 8:565–583

Longuet-Higgins MS, Stewart RW (1962) Radiation stress and mass transport in gravity waves, with application to “surf-beats”. J Fluid Mech 13:481–504

Longuet-Higgins MS, Stewart RW (1964) Radiation stresses in water waves; a physical discussion with applications. Deep-Sea Res 11:529–562

McWilliams JCM, Restrepo JM (1999) The wave-driven ocean circulation. J Phys Oceanogr 29:2523–2540

Mellor GL (2003a) The three dimensional, current and surface wave equations. J Phys Oceanogr 33:1978–1989, Also see ftp://aden.princeton.edu/pub/glm/corrected2002

Mellor GL (2003b) Users guide for a three-dimensional, primitive equation, numerical ocean model. Princeton University, Princeton, 53pp

Mellor GL (2011a) Wave radiation stress. Ocean Dyn 61:563–568

Mellor GL (2011b) Reply to Comments by A. Bennis and F. Ardhuin. J Phys Oceanogr 41:2013–2015

Mellor G, Blumberg A (2004) Wave breaking and ocean surface layer thermal response. J Phys Oceangr 34:693–698

Mellor GL, Yamada T (1982) Development of a tubulence closure model for geophysical fluid problems. Rev Geophys and Space Phys 20:851–875

Mellor GL, Donelan MA, Oey L-Y (2008) A surface wave model for coupling with numerical ocean circulation models. J Atmos Ocean Tech 35:1785–1807

Newberger PA, Allen JS (2007) Forcing a three-dimensional, hydrostatic, primitive-equation model for application in the surf zone: 2. Application to DUCK94. J Geophys Res 112:C08019. doi:10.1029/2006JC003474

Phillips OM (1977) The dynamics of the upper ocean. Cambridge University Press, Cambridge, p 336

Smith JA (2006) Wave–current interactions in finite depth. J Phys Oceanogr 36:1403–1419

Uchiyama Y, McWilliams JC, Shchepetkin AF (2010) Wave–current interaction in an oceanic circulation model with a vortex-force formalism: application to the surf zone. Ocean Modelling 34:16–35

Xu Z, Bowen AJ (1994) Wave- and wave-driven flow in water of finite depth. J Phys Oceanogr 24:1850–1866